THE JOURNAL OF BIOLOGICAL CHEMISTRY VOL. 290, NO. 10, pp. 6156–6167, March 6, 2015

Disruption of a Conserved CAP-D3 Threonine Alters Condensin Loading on Mitotic Chromosomes Leading to Chromosome Hypercondensation*

Received for publication, November 23, 2014, and in revised form, January 19, 2015 Published, JBC Papers in Press, January 20, 2015, DOI 10.1074/jbc.M114.627109

Muhammed Bakhrebah[‡§1], **Tao Zhang**[‡§1], **Jeff R. Mann**[‡§], **Paul Kalitsis**[‡§], **and Damien F. Hudson**[‡§2]

From the [‡]*Murdoch Childrens Research Institute, Royal Children's Hospital, Melbourne, Victoria 3052 and the* [§]*Department of Paediatrics, University of Melbourne, Royal Children's Hospital, Melbourne, Victoria 3052, Australia*

Background: A conserved Cdk1 site in CAP-D3 activates condensin II.
Results: Mutation of CAP-D3 Thr-1403 in chicken disrupts prophase and leads to chromosome hypercondensation.
Conclusion: Chicken CAP-D3 Thr-1403 sets the balance of chromosomal condensin I:II.
Significance: This study represents the first *in vivo* model altering the chromosomal ratio of condensin I:II and is a rare example of a mutation causing chromosome hypercondensation.

The condensin complex plays a key role in organizing mitotic chromosomes. In vertebrates, there are two condensin complexes that have independent and cooperative roles in folding mitotic chromosomes. In this study, we dissect the role of a putative Cdk1 site on the condensin II subunit CAP-D3 in chicken DT40 cells. This conserved site has been shown to activate condensin II during prophase in human cells, and facilitate further phosphorylation by polo-like kinase I. We examined the functional significance of this phosphorylation mark by mutating the orthologous site of CAP-D3 (CAP-D3^{T1403A}) in chicken DT40 cells. We show that this mutation is a gain of function mutant in chicken cells; it disrupts prophase, results in a dramatic shortening of the mitotic chromosome axis, and leads to abnormal INCENP localization. Our results imply phosphorylation of CAP-D3 acts to limit condensin II binding onto mitotic chromosomes. We present the first *in vivo* example that alters the ratio of condensin I:II on mitotic chromosomes. Our results demonstrate this ratio is a critical determinant in shaping mitotic chromosomes.

Mitotic chromosome compaction was originally visualized by the German biologist Walther Flemming, who first described the dynamics of the threadlike structures we now know as mitotic chromosomes using aniline dyes in salamander cells (1). Despite years of intensive research, how chromosomes compact to their final mitotic state is still far from clear.

Chromosome condensation is often viewed as a hierarchical series of events. In vertebrates, the interphase fiber thickens some 70-fold to a 700-nm fiber in metaphase chromosomes (2–4). At the most basic level, DNA base pairing contributes 2-fold to chromosome compaction. The histone octamer itself wraps 147 base pairs of DNA contributing to a 6–7-fold compaction and generating 10-nm fibers (5, 6). The linker histone H1 is a driver of axial shortening, and is thought to play a role in the transition from 10- to 30-nm fibers (7, 8). A cascade of histone modifications are also known to contribute to the folding of mitotic chromosomes (9). Beyond the 30-nm fiber, non-histone proteins are thought to guide the folding of DNA into mitotic chromosomes. Key members of this group of proteins (collectively termed the chromosome scaffold), are topoisomerase II, KIF4A, and the condensins (2).

In vertebrates, there are two condensin complexes, condensin I and II (10–13). Both condensins share the SMC2/SMC4 ATPase subunits that are joined by three auxiliary subunits: with CAP-H, CAP-D2, and CAP-G in condensin I, and CAP-H2, CAP-D3, and CAP-G2 in condensin II. A key distinction between the two condensins is that condensin II is present on the DNA throughout interphase and mitosis, whereas condensin I is only bound to the DNA from prometaphase to telophase (14, 15).

Studies in a variety of eukaryotes show that both condensins are essential for the correct compaction of chromosomes during mitosis, and their faithful segregation during anaphase (16–22). Localization and functional studies point to condensin II functioning from prophase, when axial shortening is most pronounced. Condensin I is not required for prophase condensation and plays a prominent role in the lateral compaction of metaphase chromosomes.

The phosphoregulation of the condensin complex is essential for its ability to compact chromosomes. It has been long established that a key factor responsible for the induction of mitotic chromosome condensation is active cyclin-dependent kinase 1 (cyclin B-Cdk1) (23). A seminal series of *in vitro* studies using *Xenopus* egg extract established that the condensins are a target of Cdk1 and this activation is an essential requirement for DNA condensation to occur (24, 25).

In general, condensins are the target of several mitotic kinases including Aurora B, Cdk1, Plk1 (Polo-like kinase)/Cdc5 (cell cycle serine threonine protein kinase 5), and CKII (casein

* This work was supported by National Health and Medical Research Council (NHMRC) Project Grants GNT1030358 and GNT1047009 and the Victorian Government's Operational Infrastructure Support Program.
[1] Both authors contributed equally to this work.
[2] To whom correspondence should be addressed: Murdoch Childrens Research Institute, Royal Children's Hospital, Melbourne, VIC 3052, Australia. Tel.: 61-3-8341-6255; E-mail: damien.hudson@mcri.edu.au.

kinase II), and evidence for their modification at multiple sites has emerged from several phosphoproteomics studies (26–28). A recent study has provided the important link between Cdk1 phosphorylation and activation of condensin II in mitosis (29). It identified a Cdk1 site at threonine 1415 in the human CAP-D3/condensin II subunit as being required to activate the complex during prophase, and allow Plk1 to be recruited along the chromosome axis. Plk1 recruitment then further phosphorylates condensin II. This key event appears an absolute requirement for correct prophase condensation. Here, we have further analyzed the functional significance of this site through its disruption in chicken DT40 cells. In agreement with the study in human HeLa cells, we found that prophase condensation is similarly altered in chicken as in human. However, we found a striking, but unreported additional phenotype: in chicken cells bearing the CAP-D3 threonine (T) 1403 to alanine (A) mutation, chromosomes became hypercondensed such that the width and length of an individual chromosome is often indistinguishable. The reason for the heightened axial compaction activity appears to be caused by condensin II overloading, thereby decreasing the ratio of condensin I:II. Our data suggest that Thr-1403 is a key site in setting the balance of condensin I and II on mitotic chromosomes.

EXPERIMENTAL PROCEDURES

Cell Culture—DT40 chicken B cells were cultured as described previously (30). CAP-D3 knock-out (KO) cells were cultured in 10 ml of medium at 39 °C and doxycycline (Dox)[3] was added to a final concentration of 200 ng/μl to repress the wild type CAP-D3 gene as previously described (17). CAP-D3 GFP cells (CAP-D3^{WT}) have been previously described (17).

Mutagenesis of CAP-D3 (T1403A) and Transfection of CAP-D3 KO—Primers (5′-CGTGCAATCAGCGCACCAGAACAGAC-3′, 3′-GTCTGTTCTGGTGCGCTGATTGCACG-5′) were selected to mutate the CAP-D3-GFP-TrAP plasmid (31) at Thr-1403, using QuikChange® Site-directed Mutagenesis kit (Agilent Technologies). CAP-D3 KO cells were co-transfected with CAP-D3^{T1403A} and blasticidin constructs by electroporation, allowed to recover for 24 h, then expanded into 96-well plates (Thermo Scientific) with blasticidin (20 μg/ml of RPMI) selection for 10–14 days. The CAP-D3 mutant clones were initially screened by a Leica DMIRB inverted microscope to detect CAP-D3 GFP signals in 96-well plates. GFP positive clones were then further screened by immunoblot using an anti-CAP-D3 antibody to select for clones expressing similar levels to parental (wild type) DT40 cells.

Pulldown Assay and Immunoblotting—Western blot was performed on cell lysates (10^6 cells) (32). Pulldown assay was performed as described before using asynchronous cells (29, 33). Antibodies used were the rabbit anti-CAP-D3 (1:2500), mouse anti-phosphothreonine-proline (1:5000, CST), mouse anti-α-tubulin (1:1000, Sigma), with goat anti-rabbit IgG-HRP and rabbit anti-mouse IgG-HRP as secondary antibodies (1:5000).

Immunofluorescence—All DT40 mitotic chromosome spreads were methanol:acetic acid fixed and prepared as described previously (34). Antibodies (dilution) used were rabbit anti-KIF4A (1:400) and rabbit anti-Topo IIα (1:400) (35). For INCENP, CENP-O, and CAP-D3 detection, cells were spun onto slides and fixed with paraformaldehyde to preserve GFP signal before co-staining with anti-INCENP (1:400) or CENP-O (1:400) (36). For CAP-H staining, cells were cytospun and processed (37) using rabbit anti-CAP-H (1:800) (38). To score prophases, cells were grown on slides and fixed (17) and stained with anti-phosphohistone H3 (Ser-10) (1:800) and anti-Lamin B1 (1:400).

Live Cell Imaging—CAP-D3^{WT} and CAP-D3^{T1403A} cells were analyzed with a live cell imaging system (DeltaVision widefield deconvolution microscope, Applied Precision, GE Healthcare) equipped with an environmental control chamber. Images were taken at 2-min intervals with three sections at each time point in 3-h movies. Images were deconvolved using DeltaVision SoftWoRx 4.1, and displayed as two-dimensional projections. The time of nuclear envelope break down (NEBD) was scored as the beginning of obvious CAP-D3-GFP foci in nuclei until either appearance of condensed chromosomes or discontinuousness of the nuclear boundary. The metaphase to anaphase time was determined from NEBD until cells with nuclei were separated into two individual cells.

Image Analysis and Microscopy—Image stacks of whole cells were taken with 0.2-μm Z-section as described previously (39). Images were deconvolved using DeltaVision SoftWoRx 4.1 and displayed as two-dimensional projections. Total CAP-D3-GFP intensity was measured for all chromosomes in the cell ($n = 10$ cells each), and also the largest chromosome (chromosome 1) from individual cells ($n = 14$) for both wild type and mutant. The intensity of fluorescence signals was measured by the Polygon function of DeltaVision SoftWoRx 4.1, and normalized to the intensity of DAPI. In summary, [CAP-D3-GFP/DAPI] = [GFP − GFP background of the same area]/[DAPI − DAPI background of the same area] and [CAP-H/DAPI] = [TRITC − TRITC background of the same area]/[DAPI − DAPI background of the same area]. Comparisons were conducted using Student's *t* test (unpaired). *p* values less than 0.05 were considered as a statistically significant difference.

RESULTS

Generation of Chicken DT40 CAP-D3^{T1403A} Mutants—Chicken CAP-D3 cDNA, and CAP-D3 conditional knock-out cells, and GFP-tagged CAP-D3 have been previously described (17, 40). The Cdk1 phosphosite at position 1403 in chicken is highly conserved in vertebrates (Fig. 1*A*). Thr-1403 was mutated to Ala-1403 in CAP-D3 cDNA, orthologous to the Cdk1 site in human CAP-D3 at Thr-1415 (29). A streptavidin-binding peptide (SBP) GFP tag was engineered into the chicken CAP-D3 DNA at the C terminus for localization and purification purposes (33). The CAP-D3-T1403A SBP-GFP construct was then transfected into CAP-D3 KO cells. GFP positive clones were selected and screened in immunoblots with CAP-D3 antibody to select for clones that expressed CAP-D3 of a similar level to parental DT40 cells (Fig. 1*B*). Five independent mutant cell lines expressing CAP-D3^{T1403A} were isolated and used for phenotypic analyses. Thereafter, we will abbreviate the CAP-D3

[3] The abbreviations used are: Dox, doxycycline; CENP-O, centromere protein O; INCENP, inner centromere protein; NEBD, nuclear envelope breakdown; SBP, streptavidin-binding peptide; Topo IIα, topoisomerase IIα.

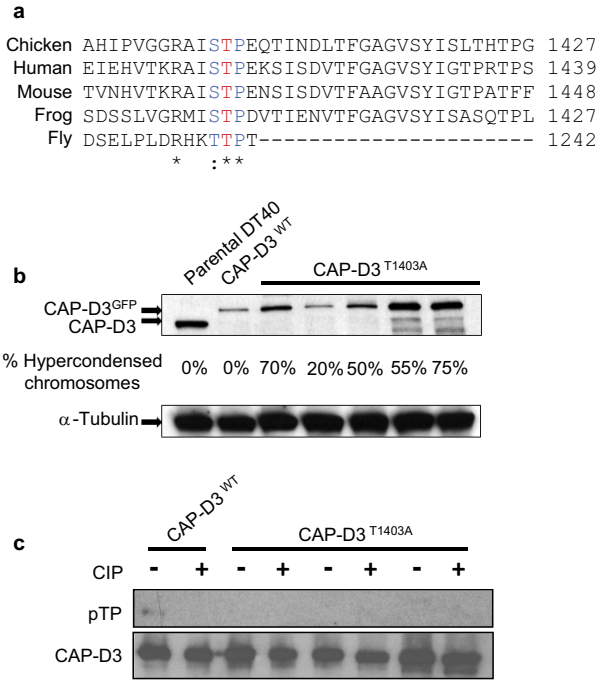

FIGURE 1. **Generation of CAP-D3^{T1403A} chicken DT40 cells.** *A*, conservation of the CAP-D3 Cdk1 site in metazoans. The conserved threonine, is highlighted in *red*. *B*, Western analysis of CAP-D3^{T1403A} mutants used in the study along side parental DT40 and CAP-D3^{WT} cells. Note, CAP-D3^{WT} and CAP-D3^{T1403A} were grown in Dox for 48 h extinguishing the untagged CAP-D3 and leaving only the tagged form (hence the band shift between parental and transgenic cell lines). The percentage of hypercondensed chromosomes is listed *below* for each cell line. *C*, pulldown analyses show Thr-1403 is a phosphosite in chicken DT40 cells. CAP-D3^{WT} and CAP-D3^{T1403A} cells were pulled down using the SBP tag and analyzed with a specific phosphothreonine-proline (*pTP*) antibody. Pulldowns were performed in duplicate with calf intestinal phosphatase (*CIP*) added to one at 37 °C for 30 min. The pTP mouse monoclonal antibody was used first and the blot was reprobed with rabbit anti-CAP-D3 antibody to confirm the specificity of the band and ensure equivalent loading.

KO CAP-D3-T1403A-SBP-GFP construct or cells to CAP-D3^{T1403A} and CAP-D3 KO WT SBP-GFP to CAP-D3^{WT}. In these cell lines, a WT untagged copy of CAP-D3 can be switched off by the addition of doxycycline (+Dox), leaving cells expressing the tagged form only. CAP-D3 KO cells without or with addition of Dox are designated CAP-D3^{ON} and CAP-D3^{OFF}, respectively.

CAP-D3^{T1403A} Does Not Affect Cell Survival but Causes a Dramatic Hypercondensation of Mitotic Chromosomes—Chicken DT40 chromosomes containing CAP-D3^{T1403A} displayed a striking phenotype. From five independent mutant clones treated with doxycycline for 48 h, spreads contained severely hypercondensed chromosomes (Fig. 2*A*). Of the five clones analyzed, the percentage of hypercondensed chromosomes present ranged from 20 to 70%, suggesting that the variation was independent of the level of CAP-D3, as judged by immunoblotting (Fig. 1*B*). To confirm that Thr-1403 is a phosphosite in chicken CAP-D3, we examined pulldowns of CAP-D3^{WT} and three independent clones of CAP-D3^{T1403A} using an antibody that recognizes the phosphorylated Cdk1 signature motif (Fig. 1*C*). The immunoblot showed a band overlapping CAP-D3 was detected by an antibody specific to phosphothreonine-proline in wild type. This band was not present in CAP-D3^{WT} pulldowns treated with phosphatase. However, no phosphoband corresponding to CAP-D3 was detected in CAP-D3^{T1403A} pulldowns, implying Thr-1403 is a phosphosite in chicken DT40 cells.

The hypercondensed chromosome phenotype was present on average 50% in (−Dox) cells (containing *both* CAP-D3 wild type transgene and CAP-D3^{T1403A}) compared with 55% (+Dox) (CAP-D3^{T1403A} only). Therefore CAP-D3^{T1403A} is a dominant mutant in chicken DT40 cells. CAP-D3^{T1403A} cells with or without Dox did not display high levels of the wiggly/curly chromosome morphology that is the hallmark phenotype of condensin II null chromosomes (17, 41). Remarkably, analysis on fixed cells also revealed no significant increase in lagging or chromosome bridges in CAP-D3^{T1403A} cells compared with wild type cells (Fig. 2*B*), despite the abnormal nature of the mitotic chromosomes.

To determine whether CAP-D3^{T1403A} affected cell survival, we added Dox to CAP-D3 KO cells expressing CAP-D3^{T1403A} over 3 days with time points taken every 24 h (Fig. 2*C*). Cells expressing only CAP-D3^{T1403A} were viable and showed similar growth rates to control cells. The growth difference when cells expressed both wild type and CAP-D3^{T1403A} (0 Dox) was indistinguishable. Thus, despite showing such abnormal chromosomes, chicken DT40 cells with CAP-D3^{T1403A} do not affect cell survival and show no obvious growth defects.

To quantitatively assess the impact of the mutation on chromosome compaction, we examined the length and width distribution of the largest chromosome between parental DT40, CAP-D3^{WT}, and CAP-D3^{T1403A} in the presence of Dox (Fig. 3). To accurately measure width and length, we stained methanol/acetic acid chromosome spreads with the scaffold marker KIF4A and counterstained with DAPI (Fig. 3, *A*–*C*). The axial stain was necessary, as often it was difficult to determine which was the axis in the hypercondensed chromosomes of CAP-D3^{T1403A} based on DNA staining alone.

Scatter plot analysis showed CAP-D3^{WT} and parental DT40 cells have a very high concordance between width and length measurements, with the distribution almost overlapping (Fig. 3*B*), confirming observations that the GFP-tagged transgene can fully rescue function. There was a striking difference between the length and width of chromosomes from CAP-D3^{T1403A} cells and parental DT40 and CAP-D3^{WT} cells. On average, CAP-D3^{T1403A} mitotic chromosomes are nearly half as long and almost twice as wide as controls. We previously reported CAP-H knock-out cells had shorter and wider chromosomes (17), suggesting the mutation in CAP-D3 produces a phenotype reminiscent, but significantly more severe than CAP-H null chromosomes.

CAP-D3^{T1403A} Shortens Prophase but Metaphase to Anaphase Proceeds Normally—The analogous mutation in human cells (CAP-D3^{T1415A}) has previously been reported to cause a disrupted prophase, curly metaphase chromosome, and severe anaphase defects; a phenotype reminiscent to removing CAP-D3 entirely (17, 29, 41). Our study also found a similar prophase defect in cells expressing CAP-D3^{T1403A}. There was a clear shortening of prophase in mutants compared with CAP-D3^{WT} cells (Fig. 4*A*). Prophase was measured as when the DNA (marked by CAP-D3 GFP) shows visible condensation until the nuclear envelope was dispersed (as seen by differential interfer-

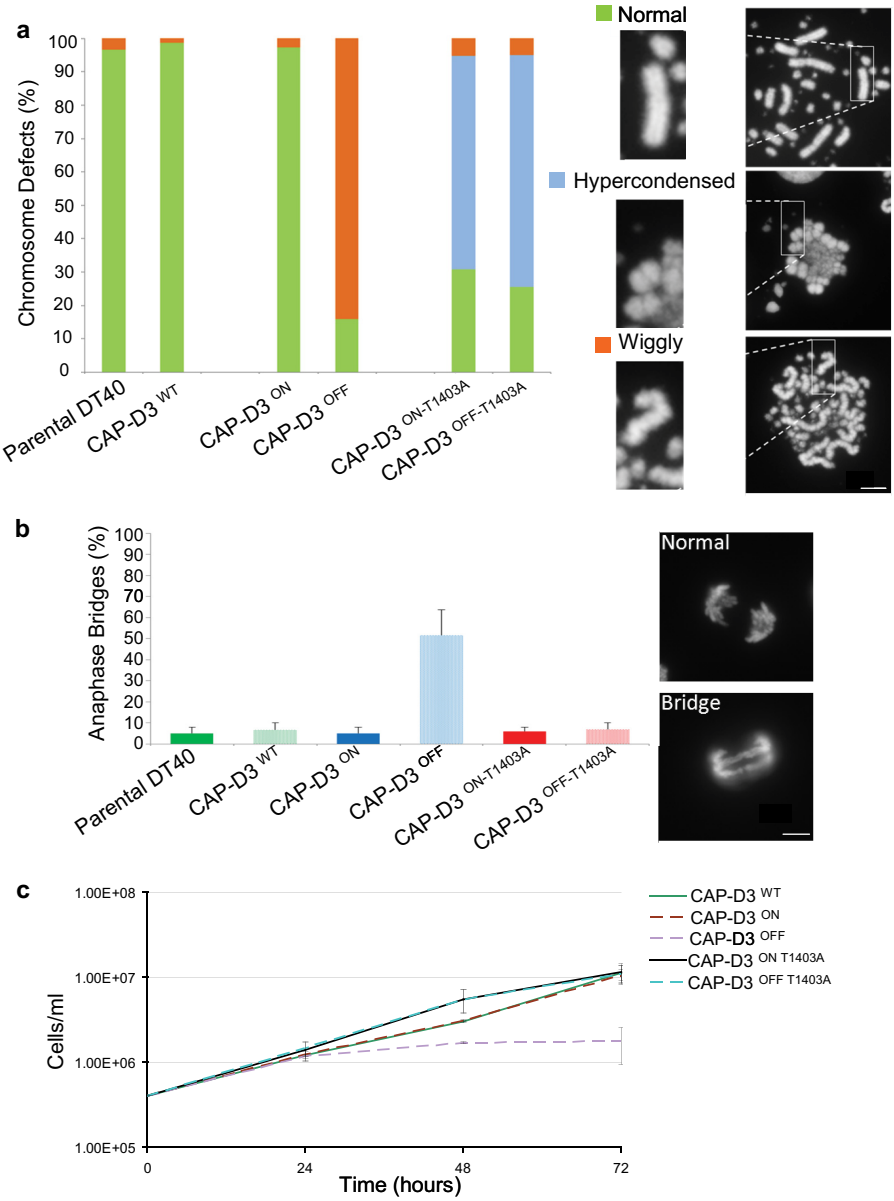

FIGURE 2. **Mutation of CAP-D3 T1403A in chicken DT40 results in hypercondensed mitotic chromosomes.** *A,* chromosome phenotypic analysis of chromosome spreads from DT40 parental, CAP-D3^{WT}, CAP-D3 KO (CAP-D3$^{ON/OFF}$), and CAP-D3^{T1403A} asynchronous cells, in the presence or absence of Dox (at 48 h +Dox for all cell lines, except for CAP-D3 KO cell line at 24 h +Dox due to cell death). A total of five independent CAP-D3^{T1403A} clones were used in the analysis. Representative images of normal, hypercondensed, and wiggly chromosomes are shown on the *right*. *Scale bar* represents 5 μm. *B,* analysis of chromosome bridge defects in WT, CAP-D3 WT^{GFP}, CAP-D3 KO, and CAP-D3^{T1403A} cell lines. Five independent CAP-D3^{T1403A} clones were used for scoring, and 20 anaphases were scored per cell line. Examples of normal and bridged anaphases are depicted on the *right*. *Scale bar* represents 5 μm. *C*, growth curves of CAP-D3 KO, CAP-D3^{WT}, and CAP-D3^{T1403A} cell lines ±Dox for 72 h, with time points taken every 24 h. Three CAP-D3^{T1403A} cell lines were used in the analysis and the plot represents the average division time for each mutant.

ence contrast microscopy). In CAP-D3^{T1403A} cells, duration of prophase lasted an average of 2 min, compared with 10 min in CAP-D3^{WT} cells (Fig. 4*B*).

Live-cell imaging also revealed that despite a shortened prophase, CAP-D3^{T1403A} cells proceed from prometaphase to anaphase with normal kinetics, taking on average ~25 min in both CAP-D3^{WT} and CAP-D3^{T1403A} (Fig. 4*B*). Also, there was no significant difference in mitotic index between wild type and mutant cells using fixed cell analysis (Fig. 4*C*). Together, these observations argue against a prolonged period in metaphase as the cause of chromosome hypercondensation. Furthermore, our live-cell imaging experiments also revealed no chromosome missegregation events in CAP-D3^{T1403A} cells, in agreement with our fixed analyses (Fig. 2*B*).

Fixed cells were also used to score prophase configurations. To detect prophase cells antibodies to lamin B1, the phosphorylation of histone H3 on serine 10 (phospho-H3) were used with DNA counterstained with DAPI (Fig. 5*A*). We divided the scoring into early and late prophase based on the amount of visible chromosome condensation. Early prophase was scored as nuclei that are showing phospho-H3 positive staining on DNA with minimal chromosome condensation, whereas late prophase was scored as nuclei that are phospho-H3 positive with clear chromosome condensation and lamin B1 intact. In

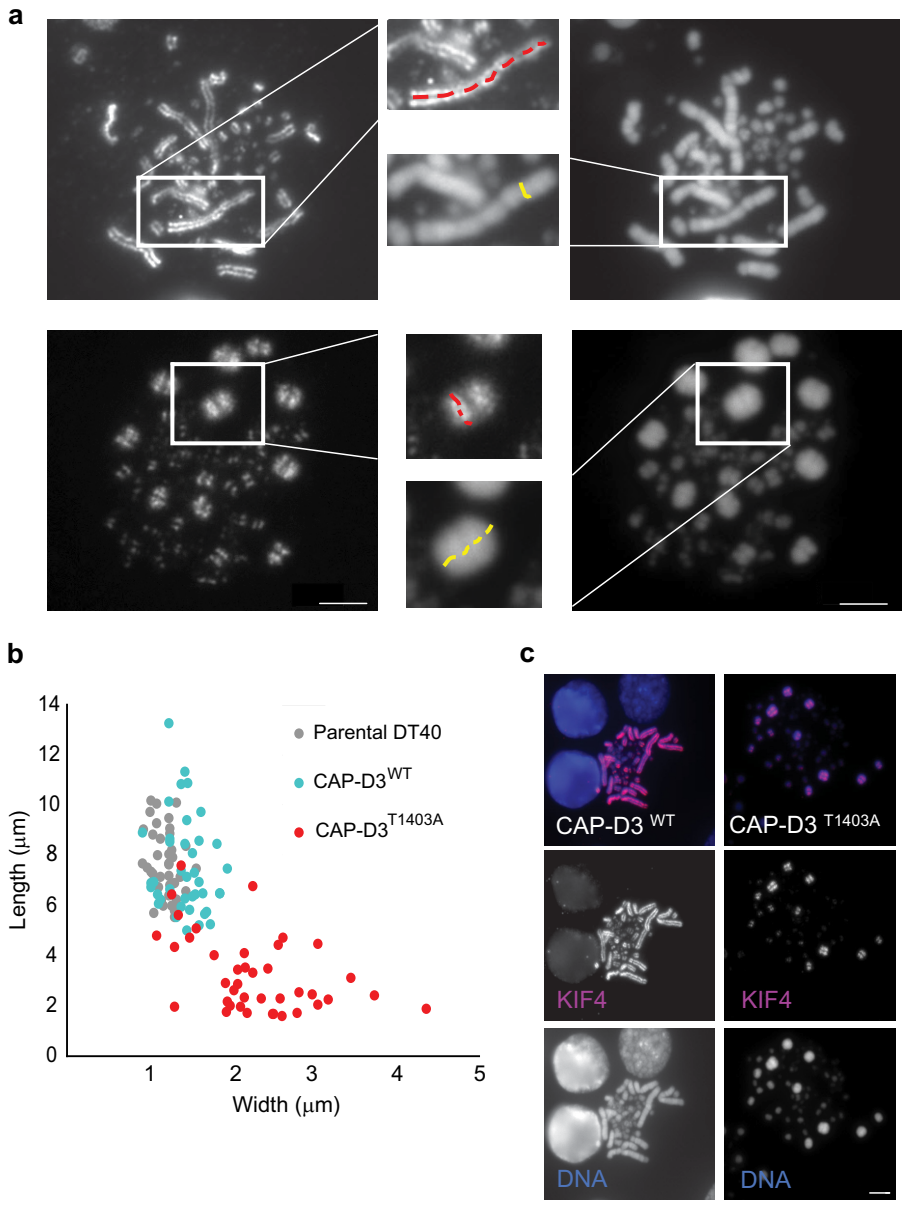

FIGURE 3. **Measurements of chromosome length and width in CAP-D3^{T1403A} cells.** *A*, the chromosomal scaffold protein KIF4A was used as a marker to identify and measure the length (axis) of mitotic chromosomes, whereas the width was measured by DNA stained with DAPI. KIF4A staining is shown on the *left panels* and DAPI on the *right panels*. For scoring purposes, the largest chromosome (chromosome 1) in each spread was measured for length using KIF4A and width using DAPI for DNA (examples in inset). *Scale bar* represents 5 μm. *B*, scatter plot analyzing parental DT40, CAP-D3^{WT}, and CAP-D3^{T1403A} chromosomes from asynchronous cells. To calculate the width and length, the longest chromosome from each spread (chromosome 1) was analyzed and plotted. Mutant and wild type cells were treated with Dox for 48 h. Two representative CAP-D3^{T1403A} clones were used. All cells were fixed with methanol:acetic acid and dropped onto slides before immunostaining with anti-KIF4A. *C*, merged example of immunofluorescence of CAP-D3^{WT} and CAP-D3^{T1403A} spreads stained with KIF4A (*red*) and DAPI (*blue*) for DNA and used for scoring in *A*.

line with our live-cell imaging (Fig. 4*A*), the CAP-D3^{T1403A} cells showed a significantly higher proportion of prophase cells with little or no condensation (Fig. 5*B*). In CAP-D3^{WT}, the reverse was true, with more prophase cells showing strong chromosome condensation. The analysis shows CAP-D3^{T1403A} mutants have a prophase equivalent to CAP-D3 null DT40 cells and agrees with findings in the orthologous CAP-D3 Cdk1 mutation in human HeLa cells (29). In general, all defects observed were present to a similar extent in either cells with only mutant CAP-D3 present (+Dox) or cells with both wild type and mutant CAP-D3 (−Dox), suggesting that in chicken DT40 cells CAP-D3^{T1403A} is a dominant-negative mutation.

CAP-D3^{T1403A} Alters the Localization of INCENP—Inner centromere protein (INCENP) is a member of the chromosome passenger complex. The complex plays key roles during mitosis including correction of faulty microtubule attachments, activation of the spindle assembly checkpoint, and orchestration of the contractile apparatus during cytokinesis (42). Under normal conditions, INCENP is transiently localized to the arms during prophase, then accumulates at the centromeres following nuclear envelope breakdown (43). Our previous work (17) showed that removing CAP-D3/condensin II alters the binding of INCENP, with the protein not concentrating at the centromeres and appearing evenly distributed along the chromosome

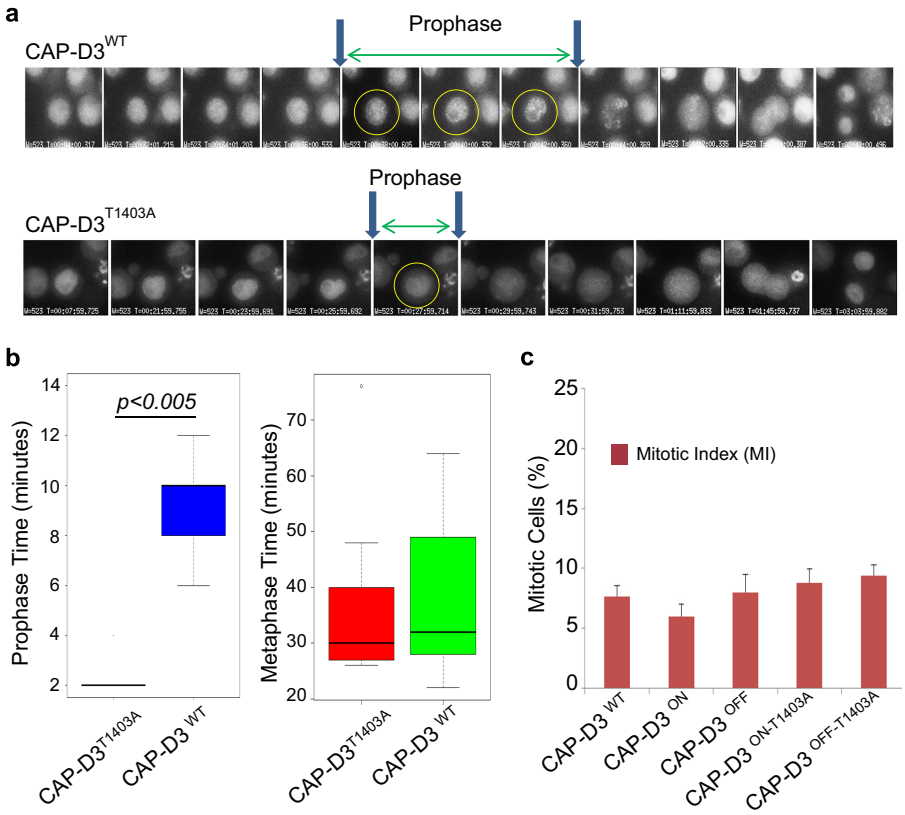

FIGURE 4. **Live cell imaging and analysis of CAP-D3^{WT} and CAP-D3^{T1403A}.** *A,* examples of CAP-D3^{WT} and CAP-D3^{T1403A} live cell imaging analysis during mitosis. Images were taken every 2 min up to prophase. After prophase, selective images are shown for metaphase, anaphase, telophase, and cytokinesis from the same movies. Note that CAP-D3^{T1403A} cells segregate chromosomes normally. *B,* quantitation of time in prophase and time from NEBD to anaphase for CAP-D3^{WT} and CAP-D3^{T1403A}. Note the very short prophase of mutant relative to wild type. There is no statistical significance between CAP-D3^{WT} and CAP-D3^{T1403A} for the metaphase to anaphase transition. *C,* the mitotic index for CAP-D3^{WT}, CAP-D3^{T1403A}, and CAP-D3 KO cells. This was calculated as the percentage of phospho-H3 positive cells from total cells. Our calculation of mitotic index includes anaphase and telophase cells. Five independent CAP-D3^{T1403A} clones were used for the scoring.

arms. As CAP-D3^{T1403A} also showed abnormal prophase kinetics (similar to CAP-D3 null cells), we reasoned that INCENP might also not accumulate on the centromeres and maintain its prophase-specific staining.

Our results showed that INCENP in CAP-D3^{T1403A} cells during metaphase appears noticeably broader, less punctate, and spread out onto the chromosome arms, rather than being concentrated at the centromeres (Fig. 6*A*). Quantitation showed 73% of CAP-D3^{T1403A} metaphases display diffuse INCENP staining at the centromere compared with 12% in CAP-D3^{WT} (p = 2.61E-04). The more diffuse staining of INCENP in CAP-D3^{T1403A} cells is likely to be a result of a shortened prophase, which may provide insufficient time for INCENP to completely transfer from the chromosome arms to the centromeres. Unlike chicken DT40 CAP-D3 null cells, INCENP in CAP-D3^{T1403A} cells is still detectable at the centromere, albeit more diffuse. These results, and previously published data (17) from our condensin II DT40 null cells, together suggest that perturbation of condensin II can disrupt the re-localization of INCENP from the chromosome arms to the centromere.

We also examined binding of the kinetochore protein CENP-O staining, which is a constitutive centromere mark in vertebrate cells (44). The staining was similar between CAP-D^{WT} and CAP-D3^{T1403A} cells (Fig. 6*B*), suggesting the kinetochore structure is not overtly compromised.

CAP-D3^{T1403A} Causes CAP-D3 to Overload Mitotic Chromosomes—It has previously been shown that removal of condensin II affects axial condensation with chromosomes becoming longer and thinner (17, 45). Therefore, we reasoned that overloading condensin II onto mitotic chromosomes might have the reverse effect; with chromosomes overcompacting and becoming significantly shorter. To test our hypothesis, we performed quantitative immunofluorescence on mutant and CAP-D3^{WT} cells using CAP-D3-GFP to assess CAP-D3 loading onto mitotic chromosomes, and also anti-CAP-H antibody for condensin I (Figs. 7, *A* and *B,* and 8, *A* and *B*). Analysis of both, total chromosomes in a given cell (Fig. 7*B, left*), and also the largest individual chromosome in that cell (Fig. 7*B, right*), showed an ~2-fold increase in the amount of CAP-D3 loaded onto CAP-D3^{T1403A} mitotic chromosomes compared with CAP-D^{WT}. There was no significant difference in the amount of CAP-D3 in interphase nuclei between CAP-D3^{T1403A} and CAP-D^{WT} (Fig. 7, *C* and *D*), suggesting mutation of the putative Cdk1 site affects mitotic chromosome condensin II loading specifically. The data provides a mechanistic insight linking mitotic chromosome hypercondensation with increased binding of CAP-D3. Conversely, CAP-H/condensin I binding is reduced on chromosomes in CAP-D3^{T1403A} compared with CAP-D3^{WT} (Fig. 8, *A* and *B*), suggesting additional CAP-D3^{T1403A} may impede the loading of condensin I. Our results therefore agree with experiments using *Xenopus* egg extracts in

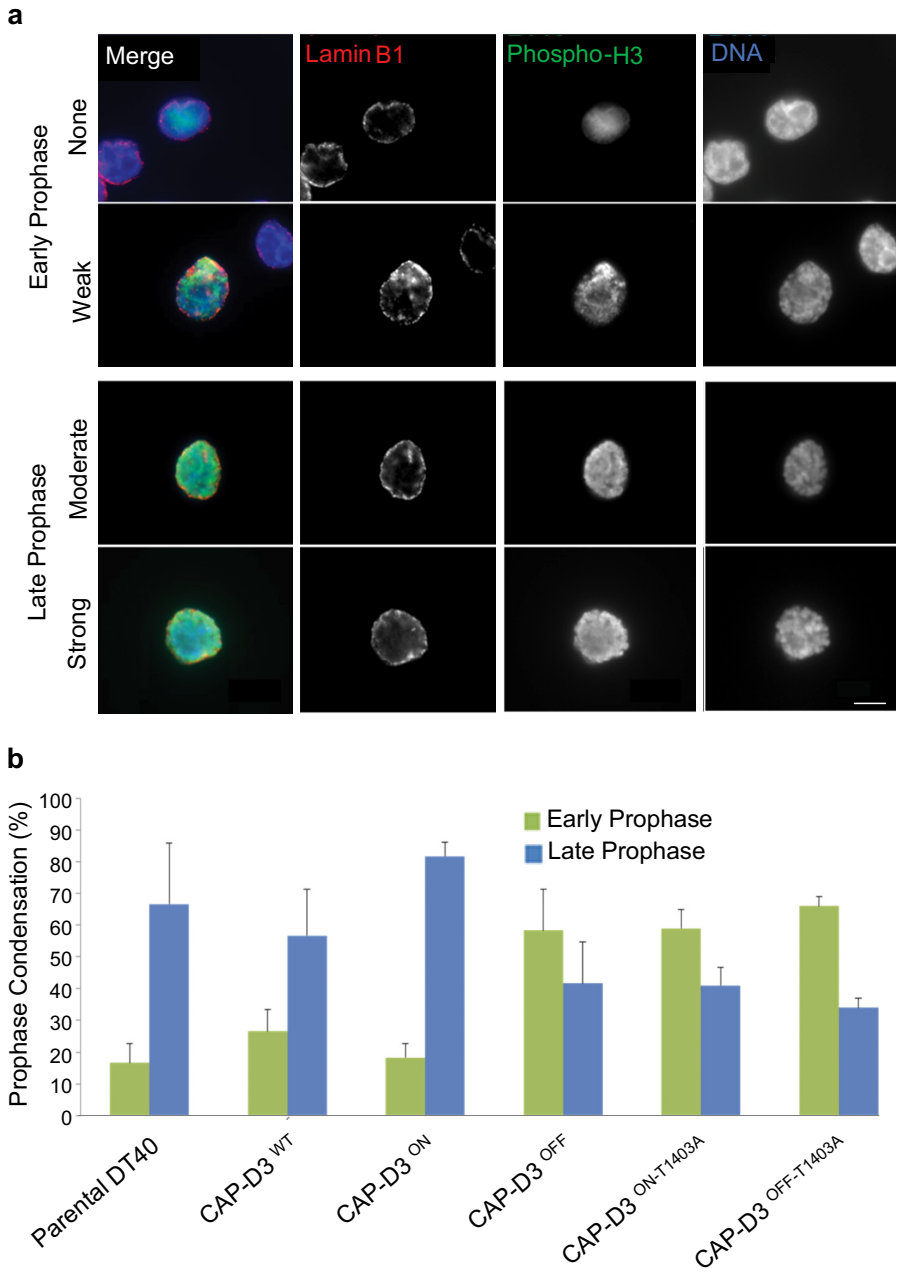

FIGURE 5. **Analysis of prophase stages using phospho-H3 staining.** *a*, cells are fixed and stained with anti-phospho-H3 serine 10 (*green*), lamin B1 (*red*), and DAPI (*blue*) for DNA. After NEBD, the nuclear envelope is dispersed, and therefore only cells with intact lamin B1 and positive for phospho-H3 are included. Prophase analysis is divided into early (with no or weak DNA condensation) and late (moderate to strong). *Scale bar* represents 5 μm. *b*, quantitation of early and late prophase images from fixed analyses for parental DT40, CAP-D3 KO, CAP-D3^{WT}, and CAP-D3^{T1403A} cells. Five independent CAP-D3^{T1403A} clones were used for the scoring and 20 prophases were scored per cell line.

a cell-free system, which show the relative ratio of condensin I to II is one of the key determinants in shaping mitotic chromosomes (45).

Topoisomerase IIα (Topo IIα) is another scaffold protein involved in the axial shortening of chromosomes and is dependent on condensin for correct localization (40, 46). Abnormal Topo IIα activity might therefore be responsible for the excessive shortening of the mitotic axes seen in CAP-D3^{T1403A} chromosomes.

To test this hypothesis, we stained for Topo IIα on CAP-D3^{WT} and CAP-D3^{T1403A} cells (Fig. 8*C*). The characteristic axial staining pattern of Topo IIα was retained in CAP-D3^{T1403A} chromosomes (Fig. 8*C*). There was a slight but statistically significant increase in the amount of Topo IIα on mutant compared with wild type mitotic chromosomes (Fig. 8*D*). However, the difference between CAP-D3^{WT} and CAP-D3^{T1403A} chromosomes for Topo IIα was not nearly as obvious as for condensin I and condensin II loading. This was reflected in both the broadly similar distribution in the scatter plot for Topo IIα binding between CAP-D3^{WT} and CAP-D3^{T1403A} and the relatively less significant value for analogous comparisons (condensin II binding $p = 7.15E-06$, condensin I binding $p = 2.18E-06$, Topo IIα binding $p = 2.15E-02$). Together, these results suggest Topo IIα might be an additive factor, but is not the driving

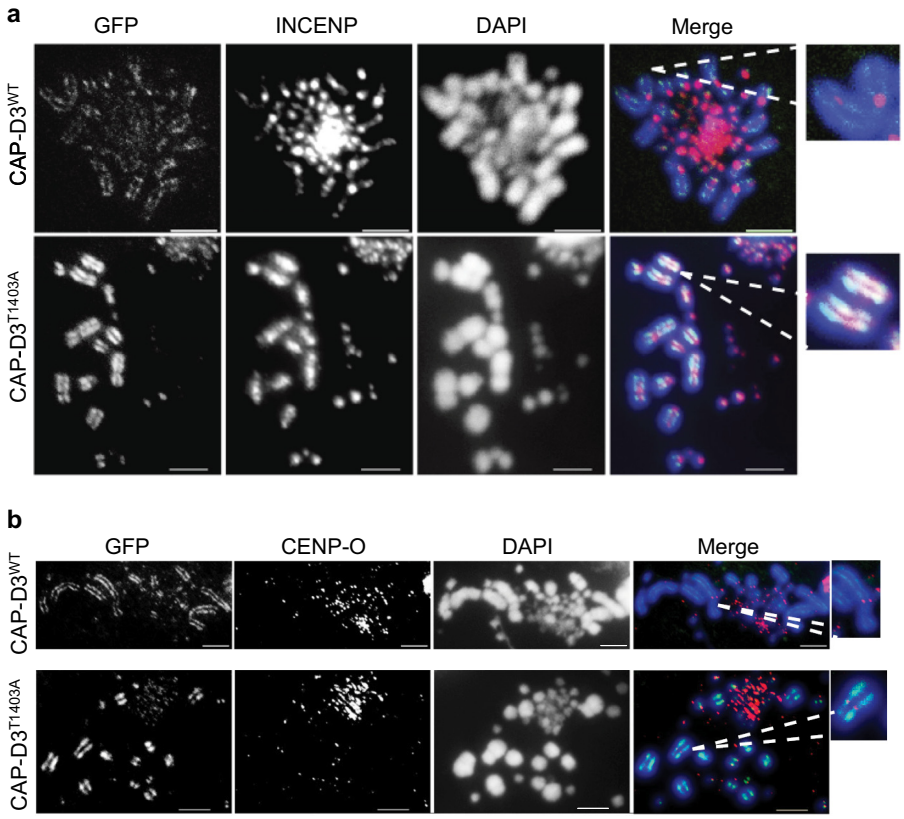

FIGURE 6. **INCENP staining is abnormal in CAP-D3^{T1403A} cells.** *A,* asynchronous CAP-D3^{WT} and CAP-D3^{T1403A} cells were grown in medium with Dox for 48 h and subjected to a hypotonic treatment, then cytospun and fixed with 4% paraformaldehyde. Cells were stained with anti-INCENP antibody (*red*), with chromosomes counterstained with DAPI (*blue*). GFP (*green*) represents CAP-D3 signal. Representative images are shown. *Scale bar* is 5 μm. *B,* asynchronous CAP-D3^{WT} and CAP-D3^{T1403A} cells were grown in medium with Dox for 24 h and subjected to a hypotonic treatment, then cytospun and fixed with 4% paraformaldehyde. Cells were stained with anti-CENP-O antibody (*red*), with chromosomes counterstained with DAPI (*blue*). GFP (*green*) represents CAP-D3 signal. Representative images are shown. *Scale bar* represents 5 μm.

factor for the chromosome hypercondensation observed in CAP-D3^{T1403A} cells.

DISCUSSION

Understanding the forces working to compact chromosomes remains a key challenge in biology. It has been clear during the last two decades that condensins are a key component of the process. Our data shed light on the significance of a key modification to the complex, and how this impacts mitotic chromosome structure. Nature has used phosphorylation as a front line tool in controlling protein regulation and function, and the task now is to understand the functional significance of these phosphosites.

The most striking result of this study is the appearance of hypercondensed chromosomes as a result of the T1403A mutation in chicken CAP-D3. At first glance, a plausible conclusion would be the shortened chromosomes seen in chicken CAP-D3^{T1403A} cells are a result of an abnormal prophase. However, in CAP-D3/condensin II null cells, there is a very abbreviated prophase but chromosomes become longer and also curlier in appearance (14, 17, 41). What is intriguing from this study is that despite a prophase equivalent to condensin II nulls, chromosomes in CAP-D3^{T1403A} cells manage to shorten their axis significantly beyond metaphase chromosomes in wild type cells. Our results show this is not the result of a prolonged period in metaphase, as is the case in of a mitotic block, where chromosomes become more condensed the longer they are blocked (20).

This work provides a molecular mechanism behind the shortened chromosomes seen in chicken CAP-D3^{T1403A} cells. Analysis of mitotic chromosomes of the CAP-D3 GFP signal, found an approximate 2-fold increase in overall CAP-D3 loading in CAP-D3^{T1403A} compared with CAP-D3^{WT}. This suggests that phosphorylation of CAP-D3 Thr-1403 might act to limit condensin II binding to mitotic chromosomes. For chicken chromosomes containing CAP-D3^{T1403A}, we envisage axial compaction is more pronounced with additional condensin II molecules loaded. This might result in further interactions between neighboring complexes. Although the ability for condensins to associate with neighboring complexes has yet to be shown *in vivo* in eukaryotic systems, it has been long hypothesized as a means to explain overall compaction and sculpting of the mitotic chromosomes (47), and has been shown *in vivo* in the bacterial condensin-like complex MukBEF (48).

Another contributing factor for the observed chromosome hypercondensation in CAP-D3^{T1403A} cells is that condensin I binding is also reduced in the mutant background, with previous studies showing when condensin I is removed chromosomes become shorter and wider (17). Condensin I binds after prophase, so one would presume this is a downstream effect of condensin II overloading. Indeed, genome-wide mapping stud-

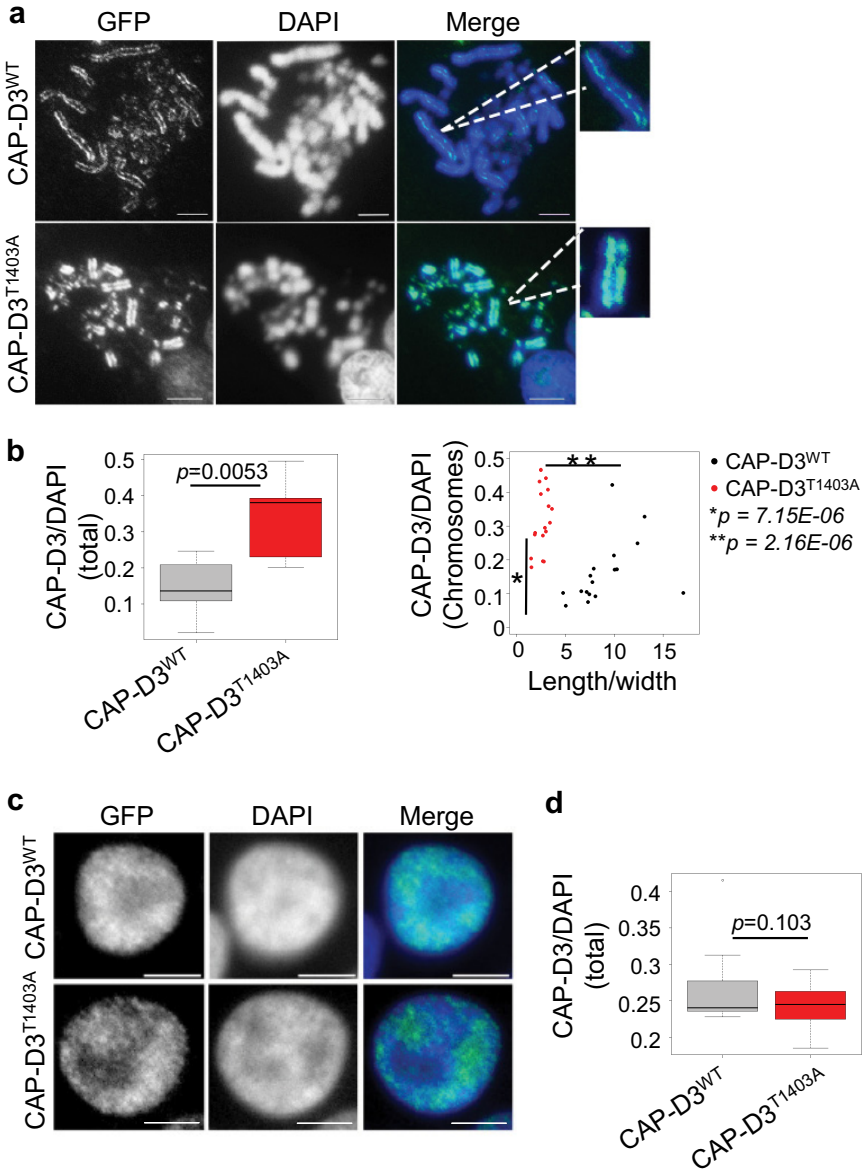

FIGURE 7. **CAP-D3 is overloaded on CAP-D3^{T1403A} mitotic chromosomes.** *A*, asynchronous CAP-D3^{WT} and CAP-D3^{T1403A} cells were grown in medium with Dox for 48 h and subjected to a hypotonic treatment, then cytospun and fixed with 4% paraformaldehyde with DNA stained with DAPI (*blue*). *Scale bar* represents 5 μm. GFP (*green*) represents CAP-D3 signal. GFP and DAPI intensity were measured as described under "Experimental Procedures." *B*, box plot are the relative intensity of CAP-D3^{WT} to DAPI of whole cells ($p = 0.0053$, $n = 10$). Scatter plot and relative intensity of CAP-D3^{WT}/DAPI of the largest individual chromosomes to the ratio of chromosome length/width ($p = 7.15E-06$ and 2.16E-08, $n = 18$). *C*, asynchronous CAP-D3^{WT} and CAP-D3^{T1403A} cells were grown in medium with Dox for 24 h and subjected to hypotonic treatment, cytospun, fixed with 4% paraformaldehyde, and the DNA stained with DAPI. *Scale bar*, 5 μm. Interphase cells were selected, GFP and DAPI intensity were measured as described under "Experimental Procedures." *D*, box plot of the relative intensity of CAP-D3-GFP to DAPI of interphase cells ($p = 0.103$, $n = 10$).

ies of condensin I and II find that they occupy different locations, but also significantly overlap (notably at promoter sequences) (32, 49, 50), although is not yet clear if condensin I and II interact directly at the same locus, or bind separately at different stages of mitosis. Whether the observed overcondensation of mitotic chromosomes is due to increased activity of condensin II or reduced activity of condensin I, or a combination of both, remains to be determined. What is clear, as previously shown *in vitro* using *Xenopus* egg extracts and naked DNA (45), is that altering the ratio of condensin I and II on chromosomes can drastically alter the shape of the mitotic chromosome. Our results confirm this conclusion *in vivo*.

A very elegant study of the biochemistry of the orthologous CAP-D3 Cdk1 site in human HeLa cells CAP-D3 has previously been published (29). Analysis of the CdK1 site and Plk1 binding box show the sites are highly conserved in human and frog (Fig. 1*A*). Our study in chicken DT40 cells found a similar prophase defect, but differed significantly in three key aspects. 1) The chicken DT40 study showed no increase in anaphase defects when the mutant CAP-D3 was expressed, whereas in the HeLa cell study, the level of chromosome missegregation in mutant cells was comparable with CAP-D3 knock-out cells. 2) The same study in HeLa cells found an increase in curly chromosomes in CAP-D3 mutant cells, which is the signature pheno-

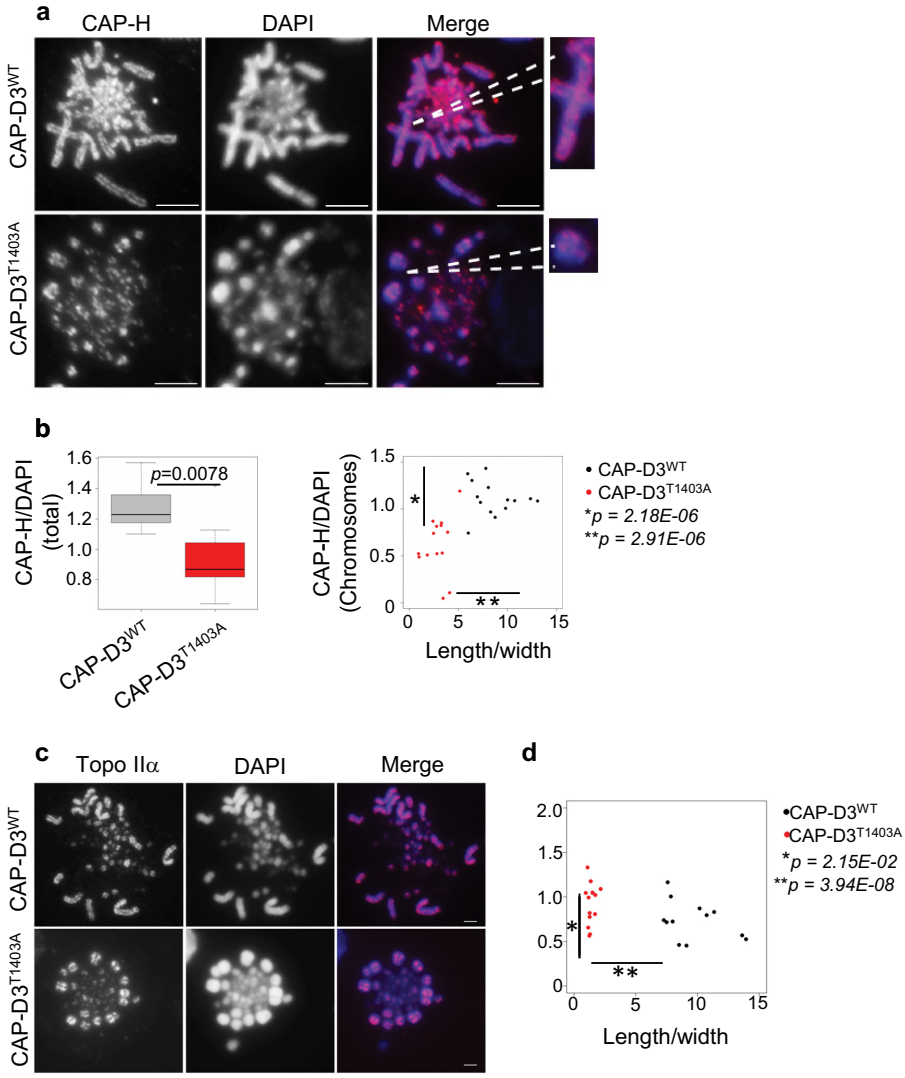

FIGURE 8. **CAP-H is reduced on CAP-D3^{T1403A} mitotic chromosomes.** *A*, asynchronous CAP-D3^{WT} and CAP-D3^{T1403A} cells were grown in medium with Dox for 48 h and subjected to a hypotonic treatment, cytospun, and stained with anti-CAP-H antibody (*red*), with chromosomes counterstained with DAPI (*blue*), *scale bar* represents 5 μm. CAP-H and DAPI intensity were measured as described under "Experimental Procedures." *B*, box plots are the relative intensity of CAP-H to DAPI of whole cells ($p = 0.0078$, $n = 10$). Scatter plot and relative intensity of CAP-H/DAPI of the largest individual chromosomes to the ratio of chromosome length/width ($p = 2.18E-05$ and $2.91E-08$, $n = 14$). *C*, representative image of Topo IIα binding in mitotic chromosome spreads of asynchronous CAP-D3^{WT} and CAP-D3^{T1403A} cells stained with Topo IIα (*red*) and DAPI (*blue*). *Scale bar*, 5 μm. *D*, scatter plot of the relative intensity of Topo IIα/DAPI of the largest individual chromosomes to the ratio of chromosome length/width ($p = 2.15E-02$, $p = 3.94E-08$, $n = 14$).

type of CAP-D3/condensin II null cells. Our study showed no increase in wiggly/curly chromosomes in the mutant. 3) The hypercondensation phenotype observed in our chicken study was not reported in the orthologous human CAP-D3 Cdk1 mutant. In general, the signature phenotypes reported in human CAP-D3 null cells (prophase condensation defect, curly/wiggly chromosomes, anaphase bridges) were also seen in the analogous mutation in CAP-D3 in human cells (CAP-D3^{T1415A}).

The differences in the phenotypes between the studies might be explained by intrinsic differences in the cell lines. One difficulty with using HeLa cells is that there is an inherent amount of chromosome instability in the derived cell line, with the reported study showing over 30% missegregation as a background level in the parental cells (29). This means teasing out phenotypes can be more difficult, as transgene expression is easily lost, resulting in a heterogeneous population of expressing cells. Therefore, RNAi knockdown might be occurring in HeLa cells not expressing the GFP-tagged CAP-D3, leading to null phenotypes. We would argue our Tet off/mutant system is a very clean and homogenous way of analyzing mutants in a cell line (chicken DT40) that has a very stable karyotype (51).

The differences between the studies might also be explained by the difference in behavior between chicken and human condensins. In chicken, quantitative proteomics has found condensin II is only 10% of total condensin in mitotic chromosomes (52), whereas in nuclear extracts of human HeLa cells, the ratio of condensin I:II is 1:1 (41). As defined using a cell-free system in *Xenopus*, the ratio of condensin I:II is 5:1 (45). The difference in ratio between species could mean the behavior of the condensins alters in different species in response to different post-translational modifications such as the phosphorylation of CAP-D3 at Thr-1403. Indeed, it is not unprecedented in metazoans to show species-specific differences in condensin behav-

ior. For instance, in *Drosophila*, condensin I accumulates in prophase when there are visible signs of condensation (53), whereas all other metazoans examined show condensin I only binds DNA after NEBD (14, 15, 19). Therefore, differences in behavior of the condensins across vertebrate classes are not unexpected. Furthermore, although the orthologous site in human is phosphorylated by Cdk1 and our own data show Thr-1403 is a phosphosite, phosphorylation specifically by Cdk1 at CAP-D3 Thr-1403 in chicken DT40 cells needs to be further confirmed. Future studies will address whether the cascade of Cdk1-mediated Plk1 hyperphosphorylation of condensin II subunits seen in human, is conserved in chicken and other vertebrates.

Our study identifies a key site in CAP-D3 in chicken DT40 cells that helps lock condensation levels. This fits in with our belief that condensin II acts to determine mitotic chromosome rigidity by establishing a scaffold axis during prophase (17). Fluorescence recovery after photobleaching data show condensin II is significantly more stable on mitotic chromosomes than condensin I (14). The observed stability of condensin II supports a model of establishing a scaffold upon which the mitotic chromosome is built. Our data in chicken suggest that phosphorylation of CAP-D3 Thr-1403 might act to seal this lock by establishing a threshold level for condensin II binding mitotic chromosomes.

This work shows that condensins act to establish and also to *maintain* chromosome condensation levels, as pioneering experiments using *in vitro* assays have suggested (54). We show that altering a residue on the condensin II complex can drastically alter the activity of the complex and result in a gain of function mutation leading to chromosome hypercondensation. This is a rare example of a mutation that causes chromosome hypercondensation, which is not the result of a prometaphase arrest. A chemically induced mutation of the catalytic subunit of protein phosphatase 1 in *Drosophila* also produces hypercondensed chromosomes (55), but to our knowledge there are no other reported examples. Future studies will reveal if the chromosome hypercondensation phenotype of this conserved Cdk1 site is observed in other species aside from chicken. What is clear is that Thr-1403 is a key and essential requirement for prophase condensation, and an essential modulator of condensin II function.

Acknowledgment—We thank Kathryn Marshall for help in preparation of the manuscript and figures.

REFERENCES

1. Flemming, W. (1878) Zur Kenntniss der Zelle und ihrer Theilungs-Erscheinungen. *Schriften des Naturwissenschaftlichen Vereins für Schleswig-Holstein* **3,** 23–27
2. Belmont, A. S. (2006) Mitotic chromosome structure and condensation. *Curr. Opin. Cell Biol.* **18,** 632–638
3. Moser, S. C., and Swedlow, J. R. (2011) How to be a mitotic chromosome. *Chromosome Res.* **19,** 307–319
4. Vagnarelli, P. (2012) Mitotic chromosome condensation in vertebrates. *Exp. Cell Res.* **318,** 1435–1441
5. Kornberg, R. D. (1974) Chromatin structure: a repeating unit of histones and DNA. *Science* **184,** 868–871
6. Saitoh, N., Goldberg, I. G., Wood, E. R., and Earnshaw, W. C. (1994) ScII: an abundant chromosome scaffold protein is a member of a family of putative ATPases with an unusual predicted tertiary structure. *J. Cell Biol.* **127,** 303–318
7. Maeshima, K., Imai, R., Tamura, S., and Nozaki, T. (2014) Chromatin as dynamic 10-nm fibers. *Chromosoma* **123,** 225–237
8. Maresca, T. J., Freedman, B. S., and Heald, R. (2005) Histone H1 is essential for mitotic chromosome architecture and segregation in *Xenopus laevis* egg extracts. *J. Cell Biol.* **169,** 859–869
9. Wilkins, B. J., Rall, N. A., Ostwal, Y., Kruitwagen, T., Hiragami-Hamada, K., Winkler, M., Barral, Y., Fischle, W., and Neumann, H. (2014) A cascade of histone modifications induces chromatin condensation in mitosis. *Science* **343,** 77–80
10. Aragon, L., Martinez-Perez, E., and Merkenschlager, M. (2013) Condensin, cohesin and the control of chromatin states. *Curr. Opin. Genet. Dev.* **23,** 204–211
11. Hirano, T. (2012) Condensins: universal organizers of chromosomes with diverse functions. *Genes Dev.* **26,** 1659–1678
12. Piazza, I., Haering, C. H., and Rutkowska, A. (2013) Condensin: crafting the chromosome landscape. *Chromosoma* **122,** 175–190
13. Hudson, D. F., Marshall, K. M., and Earnshaw, W. C. (2009) Condensin: architect of mitotic chromosomes. *Chromosome Res.* **17,** 131–144
14. Gerlich, D., Hirota, T., Koch, B., Peters, J. M., and Ellenberg, J. (2006) Condensin I stabilizes chromosomes mechanically through a dynamic interaction in live cells. *Curr. Biol.* **16,** 333–344
15. Ono, T., Fang, Y., Spector, D. L., and Hirano, T. (2004) Spatial and temporal regulation of condensins I and II in mitotic chromosome assembly in human cells. *Mol. Biol. Cell* **15,** 3296–3308
16. Dej, K. J., Ahn, C., and Orr-Weaver, T. L. (2004) Mutations in the *Drosophila* condensin subunit dCAP-G: defining the role of condensin for chromosome condensation in mitosis and gene expression in interphase. *Genetics* **168,** 895–906
17. Green, L. C., Kalitsis, P., Chang, T. M., Cipetic, M., Kim, J. H., Marshall, O., Turnbull, L., Whitchurch, C. B., Vagnarelli, P., Samejima, K., Earnshaw, W. C., Choo, K. H., and Hudson, D. F. (2012) Contrasting roles of condensin I and condensin II in mitotic chromosome formation. *J. Cell Sci.* **125,** 1591–1604
18. Hagstrom, K. A., Holmes, V. F., Cozzarelli, N. R., and Meyer, B. J. (2002) *C. elegans* condensin promotes mitotic chromosome architecture, centromere organization, and sister chromatid segregation during mitosis and meiosis. *Genes Dev.* **16,** 729–742
19. Hirota, T., Gerlich, D., Koch, B., Ellenberg, J., and Peters, J.-M. (2004) Distinct functions of condensin I and II in mitotic chromosome assembly. *J. Cell Sci.* **117,** 6435–6445
20. Hudson, D. F., Vagnarelli, P., Gassmann, R., and Earnshaw, W. C. (2003) Condensin is required for nonhistone protein assembly and structural integrity of vertebrate mitotic chromosomes. *Dev. Cell* **5,** 323–336
21. Strunnikov, A. V., Hogan, E., and Koshland, D. (1995) SMC2, a *Saccharomyces cerevisiae* gene essential for chromosome segregation and condensation, defines a subgroup within the SMC family. *Genes Dev.* **9,** 587–599
22. Hirano, T., Funahashi, S., Uemura, T., and Yanagida, M. (1986) Isolation and characterization of *Schizosaccharomyces pombe* cutmutants that block nuclear division but not cytokinesis. *EMBO J.* **5,** 2973–2979
23. Gurdon, J. B. (1968) Changes in somatic cell nuclei inserted into growing and maturing amphibian oocytes. *J. Embryol. Exp. Morphol.* **20,** 401–414
24. Kimura, K., Hirano, M., Kobayashi, R., and Hirano, T. (1998) Phosphorylation and activation of 13S condensin by Cdc2 *in vitro*. *Science* **282,** 487–490
25. Kimura, K., Cuvier, O., and Hirano, T. (2001) Chromosome condensation by a human condensin complex in *Xenopus* egg extracts. *J. Biol. Chem.* **276,** 5417–5420
26. Lavoie, B. D., Hogan, E., and Koshland, D. (2004) *In vivo* requirements for rDNA chromosome condensation reveal two cell-cycle-regulated pathways for mitotic chromosome folding. *Genes Dev.* **18,** 76–87
27. Lipp, J. J., Hirota, T., Poser, I., and Peters, J. M. (2007) Aurora B controls the association of condensin I but not condensin II with mitotic chromosomes. *J. Cell Sci.* **120,** 1245–1255
28. Takemoto, A., Murayama, A., Katano, M., Urano, T., Furukawa, K., Yokoyama, S., Yanagisawa, J., Hanaoka, F., and Kimura, K. (2007) Analysis

of the role of Aurora B on the chromosomal targeting of condensin I. *Nucleic Acids Res.* **35,** 2403–2412
29. Abe, S., Nagasaka, K., Hirayama, Y., Kozuka-Hata, H., Oyama, M., Aoyagi, Y., Obuse, C., and Hirota, T. (2011) The initial phase of chromosome condensation requires Cdk1-mediated phosphorylation of the CAP-D3 subunit of condensin II. *Genes Dev.* **25,** 863–874
30. Buerstedde, J.-M., and Takeda, S. (1991) Increased ratio of targeted to random integration after transfection of chicken B cell lines. *Cell* **67,** 179–188
31. Hudson, D. F., Ohta, S., Freisinger, T., Macisaac, F., Sennels, L., Alves, F., Lai, F., Kerr, A., Rappsilber, J., and Earnshaw, W. C. (2008) Molecular and genetic analysis of condensin function in vertebrate cells. *Mol. Biol. Cell* **19,** 3070–3079
32. Kim, J. H., Zhang, T., Wong, N. C., Davidson, N., Maksimovic, J., Oshlack, A., Earnshaw, W. C., Kalitsis, P., and Hudson, D. F. (2013) Condensin I associates with structural and gene regulatory regions in vertebrate chromosomes. *Nat. Commun.* **4,** 2537
33. Kim, J. H., Chang, T. M., Graham, A. N., Choo, K. H., Kalitsis, P., and Hudson, D. F. (2010) Streptavidin-binding peptide (SBP)-tagged SMC2 allows single-step affinity fluorescence, blotting or purification of the condensin complex. *BMC Biochem.* **11,** 50
34. Earnshaw, W. C., Ratrie, H., 3rd, and Stetten, G. (1989) Visualization of centromere proteins CENP-B and CENP-C on a stable dicentric chromosome in cytological spreads. *Chromosoma* **98,** 1–12
35. Samejima, K., Ogawa, H., Cooke, C. A., Hudson, D., Macisaac, F., Ribeiro, S. A., Vagnarelli, P., Cardinale, S., Kerr, A., Lai, F., Ruchaud, S., Yue, Z., and Earnshaw, W. C. (2008) A promoter-hijack strategy for conditional shutdown of multiply spliced essential cell cycle genes. *Proc. Natl. Acad. Sci. U.S.A.* **105,** 2457–2462
36. Kwon, M. S., Hori, T., Okada, M., and Fukagawa, T. (2007) CENP-C is involved in chromosome segregation, mitotic checkpoint function, and kinetochore assembly. *Mol. Biol. Cell* **18,** 2155–2168
37. Warburton, P. E., Cooke, C. A., Bourassa, S., Vafa, O., Sullivan, B. A., Stetten, G., Gimelli, G., Warburton, D., Tyler-Smith, C., Sullivan, K. F., Poirier, G. G., and Earnshaw, W. C. (1997) Immunolocalization of CENP-A suggests a distinct nucleosome structure at the inner kinetochore plate of active centromeres. *Curr. Biol.* **7,** 901–904
38. Vagnarelli, P., Hudson, D. F., Ribeiro, S. A., Trinkle-Mulcahy, L., Spence, J. M., Lai, F., Farr, C. J., Lamond, A. I., and Earnshaw, W. C. (2006) Condensin and Repo-Man-PP1 co-operate in the regulation of chromosome architecture during mitosis. *Nat. Cell. Biol.* **8,** 1133–1142
39. Chen, H., Hughes, D. D., Chan, T. A., Sedat, J. W., and Agard, D. A. (1996) IVE (Image Visualization Environment): a software platform for all three-dimensional microscopy applications. *J. Struct. Biol.* **116,** 56–60
40. Samejima, K., Samejima, I., Vagnarelli, P., Ogawa, H., Vargiu, G., Kelly, D. A., de Lima Alves, F., Kerr, A., Green, L. C., Hudson, D. F., Ohta, S., Cooke, C. A., Farr, C. J., Rappsilber, J., and Earnshaw, W. C. (2012) Mitotic chromosomes are compacted laterally by KIF4 and condensin and axially by topoisomerase IIα. *J. Cell Biol.* **199,** 755–770
41. Ono, T., Losada, A., Hirano, M., Myers, M. P., Neuwald, A. F., and Hirano, T. (2003) Differential contributions of condensin I and condensin II to mitotic chromosome architecture in vertebrate cells. *Cell* **115,** 109–121
42. Carmena, M., Wheelock, M., Funabiki, H., and Earnshaw, W. C. (2012) The chromosomal passenger complex (CPC): from easy rider to the godfather of mitosis. *Nat. Rev. Mol. Cell Biol.* **13,** 789–803
43. Ruchaud, S., Carmena, M., and Earnshaw, W. C. (2007) Chromosomal passengers: conducting cell division. *Nat. Rev. Mol. Cell Biol.* **8,** 798–812
44. Hori, T., Okada, M., Maenaka, K., and Fukagawa, T. (2008) CENP-O class proteins form a stable complex and are required for proper kinetochore function. *Mol. Biol. Cell* **19,** 843–854
45. Shintomi, K., and Hirano, T. (2011) The relative ratio of condensin I to II determines chromosome shapes. *Genes Dev.* **25,** 1464–1469
46. Farr, C. J., Antoniou-Kourounioti, M., Mimmack, M. L., Volkov, A., and Porter, A. C. (2014) The α isoform of topoisomerase II is required for hypercompaction of mitotic chromosomes in human cells. *Nucleic Acids Res.* **42,** 4414–4426
47. Hirano, T. (2006) At the heart of the chromosome: SMC proteins in action. *Nat. Rev. Mol. Cell Biol.* **7,** 311–322
48. Badrinarayanan, A., Reyes-Lamothe, R., Uphoff, S., Leake, M. C., and Sherratt, D. J. (2012) *In vivo* architecture and action of bacterial structural maintenance of chromosome proteins. *Science* **338,** 528–531
49. Dowen, J. M., Bilodeau, S., Orlando, D. A., Hübner, M. R., Abraham, B. J., Spector, D. L., and Young, R. A. (2013) Multiple structural maintenance of chromosome complexes at transcriptional regulatory elements. *Stem Cell Reports* **1,** 371–378
50. Kranz, A. L., Jiao, C. Y., Winterkorn, L. H., Albritton, S. E., Kramer, M., and Ercan, S. (2013) Genome-wide analysis of condensin binding in *Caenorhabditis elegans*. *Genome Biol.* **14,** R112
51. Hudson, D. F., Morrison, C., Ruchaud, S., and Earnshaw, W. C. (2002) Reverse genetics of essential genes in tissue-culture cells: "dead cells talking". *Trends Cell Biol.* **12,** 281–287
52. Ohta, S., Bukowski-Wills, J. C., Sanchez-Pulido, L., Alves Fde, L., Wood, L., Chen, Z. A., Platani, M., Fischer, L., Hudson, D. F., Ponting, C. P., Fukagawa, T., Earnshaw, W. C., and Rappsilber, J. (2010) The protein composition of mitotic chromosomes determined using multiclassifier combinatorial proteomics. *Cell* **142,** 810–821
53. Oliveira, R. A., Heidmann, S., and Sunkel, C. E. (2007) Condensin I binds chromatin early in prophase and displays a highly dynamic association with *Drosophila* mitotic chromosomes. *Chromosoma* **116,** 259–274
54. Hirano, T., Kobayashi, R., and Hirano, M. (1997) Condensins, chromosome condensation protein complexes containing XCAP-C, XCAP-E and a *Xenopus* homolog of the *Drosophila* Barren protein. *Cell* **89,** 511–521
55. Baksa, K., Morawietz, H., Dombrádi, V., Axton, M., Taubert, H., Szabo, G., Török, I., Udvardy, A., Gyurkovics, H., and Szöör, B. (1993) Mutations in the protein phosphatase 1 gene at 87B can differentially affect suppression of position-effect variegation and mitosis in *Drosophila melanogaster*. *Genetics* **135,** 117–125